ISSN-1996-918X

Pak. J. Anal. Environ. Chem. Vol. 27, No. 1 (2026) 470691c

http://doi.org/10.21743/pjaec/2026/470691c

Synthesis and Characterization of polypyrrole / Silver Nanoparticles Composites as Creatinine Sensor

Ammar M. Abdullah* and Ibraheem J. Ibraheem

Department of Chemistry, College of Science, University of Anbar, Ramadi, Al Anbar, Iraq.

*Corresponding author Email:ammar.moh@uoanbar.edu.iq

Received 10 July 2025, Revised 17 March 2026, Accepted 02 April 2026

Academic Editor: Amber R. Solangi

Abstract

The Jaffe reaction is commonly employed to detect creatinine. This work involves the creation of several electrochemical sensors for the detection of creatinine, utilizing films made from polymer composites with nanoparticles and picric acid. Based on the interaction mechanism of creatinine, we synthesized four working electrodes (WEs): polypyrrole (Ppy) alone, Ppy with silver nanoparticles (AgNPs), Ppy with picric acid, and a combination of Ppy, picric acid, and AgNPs. All these electrochemical sensors exhibited distinctive sensitivities for creatinine detection. The performance and electrochemical behavior of the sensors were evaluated using cyclic voltammetry. AgNPs were synthesized biologically using Capsicum annuum leaves extract, serving as both a reducing and capping agent. Ppy was prepared via chemical polymerization using ammonium persulfate (APS) as an oxidizing agent in the presence of hydrochloric acid as a dopant. The sensor presented a limit of detection (LOD) of 0.144 mg/dL and a limit of quantification (LOQ) of 0.44 mg/dL. Ppy and AgNPs were characterized by UV-Visible spectroscopy, field emission scanning electron microscopy (FESEM), atomic force microscopy (AFM), and X-ray diffraction (XRD). The prepared sensors were successfully applied for the direct detection of creatinine.

Keywords: Creatinine, Biosensor, Silver nanoparticles, Picric acid, Polypyrrole.

Introduction

Polypyrrole (Ppy) is an electrically conducting polymer. It consists of heterocyclic monomers linked to each other. The molecular structure includes a five-membered pyrrole ring linked together at the 2 and 5 positions. It was first prepared in 1963 from tetraiodopyrrole by pyrolysis [1]. Ppy is a naturally occurring conducting polymer that is frequently used as a biomaterial because of its exceptional qualities, which include stability, electrical conductivity, and exceptional biocompatibility [2]. Because of its low cost and strong electrical properties, Ppy is the most extensively used in the biomedical field as well as other areas, including sensors, actuators, and energy generators (batteries and solar cells) [3]. Is the most widely used method for easily and quickly synthesizing Ppy without the need for specialized equipment. Large-scale production can also be accomplished with this technology. Black powder of Ppy may be prepared by the oxidation of Ppy with chemical oxidants [4]. Conducting polymers (CPs) received great interest due to their economic significance, strong environmental stability and electrical conductivity, and also because of their valuable mechanical, optical, and electronic features [5]. Since their discovery, researchers have been investigating the unique electrical

characteristics of intrinsically conductive polymers for a variety of applications. Because of their conjugated electron backbone, these polymers have electrical properties like low ionization potential, low energy optical transmission, and strong electron affinities [6]. The synthesis of nanoparticles by biological processes is categorized under the bottom-up strategy, wherein reduction is facilitated by stabilizing agents. The biosynthetic method is a clean, non-toxic, and environmentally friendly methodology for nanoparticles creation under atmospheric circumstances [7]. Plant-mediated preparation has garnered considerable interest due to the quantity and diversity of plant species, which offer a substantial reservoir of bioactive chemicals for nanoparticle synthesis [8, 9]. Peppers (Capsicum spp.) are regarded as possessing significant nutritional value due to their phytochemical content. Peppers are rich in phytochemicals, including carotenoids, capsaicinoids, flavonoids, ascorbic acids, anthocyanins, vitamins, phenolic acids, and tocopherols [10-12]. AgNPs have been much studied because of their unique properties, which include their optical, electrical, and antimicrobial properties [13]. Compared to other metals, silver has a low chemical reactivity and great stability, making it an important nano-technology invention. Since AgNPs have special physicochemical features, they have drawn a lot of interest in biological applications [14]. Which make them distinct substances with antibacterial, antifungal, antiviral, and anticancer activities [15]. Additionally, AgNPs are playing a significant function for many uses, including information storage, chemical sensing, ointments, nanomedicine, antioxidants, anti-microbial agents, and the food sector [16]. The macroscopic materials known as composites are created when two or more materials with dissimilar morphologies, compositions, and physical and chemical characteristics are combined. These materials acquire new or enhanced mechanical, chemical, physical, and other qualities that do not correspond to their constituent parts [17]. Composites can be made to meet precise geometrical, structural, mechanical, chemical, and even aesthetic requirements, depending on the intended use. These artificial materials are used in a variety of industries and fields, including aerospace, naval (such as ships and boats), automotive (such as automobile bodies), construction (like buildings and bridges), and biomedical [18]. The nanocomposites have good activity against different gram +ve and gram –ve bacterium kinds and distinct inhibition of breast cancer cells [19]. Biosensors are analytical instruments that integrate a biological element with a physicochemical sensor [20]. These technologies can deliver rapid, dependable, and precise identification of particular biological processes and analytes [21]. Biosensors can be classified as electrochemical, optical, thermal, or piezoelectric based on the type of transducer utilized [22].

Electrochemical diagnostics typically have exceptional attributes, including high sensitivity, an extensive detection range, cost-effectiveness, and ease of delivery [23]. An electrochemical biosensor is an autonomous, consolidated apparatus that delivers certain quantifiable or semi-quantifiable analytical data utilizing a biological recognition element (biochemical receptor) in connection with an electrochemical transduction component [24]. Biological constituents serve as sensitive elements; the electrode functions as a conversion component; and current, potential, and resistance are the measurable qualities of a signal. They have benefits like improved sensitivity, durability, dependability, and the possibility of integration onto a single chip [25].

The electrochemical biosensor is a sensing platform that assesses variations in electrical characteristics (current, impedance, conductivity, voltage, or potential signal) resulting from biochemical interactions between a biomolecular component and a target analyte [26]. The clinical diagnosis of renal dysfunction, acute kidney injury, or chronic kidney disease is conducted by assessing creatinine levels in human serum. Creatinine is a metabolic byproduct of muscle, generated by the conversion of creatine and creatine phosphate, accompanied by the release of energy [27]. Electrochemical creatinine (bio) sensors are a feasible substitute for traditional analytical techniques and clinical methodologies [28]. Electrochemical biosensors are autonomous integrated devices that deliver specific quantitative or semi-quantitative analytical data utilizing a biological recognition element (biochemical receptor) in direct contact with an electrochemical transduction element [29].

Gao *et al.* established a novel Cr detection method by altering glassy carbon electrodes with electrodeposited copper nanoparticles on the polydopamine-reduced graphene oxide-nano bead layer. Square-wave voltammetry was employed to identify Cr in a phosphate buffer solution (PBS). The sensor demonstrated elevated sensitivity, a linear response range of 0.01–100 µM, and a detection limit of 2 nM [30]. Pedrozo-Peñafiel *et al.* utilized a gold electrode altered with Nafion and graphene quantum dots in a Cu^{2+} distribution to develop a voltammetric sensor for the sensing of Cr in urine examples. This sensor exhibited a variable reaction range of 0.11–50.9 mg/L; conversely, its selectivity was diminished [31]. Sriramprabha *et al.* synthesised Fe_2O_3 /polyaniline nanocomposite for the sensing of Cr in a sample. A response series of 0.001-13 Mm and a detection limit of 144 nM with improved sensitivity were reported. The sensor operated without the necessity of a bioreceptor or binder, nor did it require any pre-treatment of the material [32]. Fava *et al.* developed a screen-printed device modified with carbon black film for the non-enzymatic creatinine determination based on its complex formation with Fe(III). Cyclic voltammetry and differential pulse voltammetry were utilized for the electrochemical characterization and analytical performance assessment of the microcell. The sensor exhibited a linear response for creatinine concentrations between 0.10 and 6.5 mmol L^{-1}, with a detection limit of 0.043 mmol L^{-1}. [33].

In this research, an electrochemical sensor was prepared and used to detect creatinine directly by recording the response of the direct interaction of creatinine with the used electrode.

Material and Methods

Materials and Chemicals

Fresh leaves of Capsicum annuum were collected from Saqlawia, Anbar, Iraq; silver nitrate and pyrrole were purchased from Sigma-Aldrich (USA); acetone and ethanol from Scharlau (Spain); ammonium persulfate from Prolabo (France), hydrochloric acid from CDH (India), and creatinine were procured from Alpha Chemika (India).

Instrumentations

All electrochemical measurements were conducted with a potentiostat apparatus. A three-electrodes system, was used comprising a modified ITO electrode with Ppy, Ppy /picric acid, Ppy/AgNPs and Ppy/picric acid/AgNPs as the working electrodes, a saturated calomel electrode (SCE) as the reference electrode, and a platinum wire as the counter electrode. The following techniques were used to determine the structure of the

nanoparticles: atomic force microscopy (AFM), field emission scanning electron microscopy (FE-SEM) (AxiaChemiSEM), FTIR spectroscopy (Shimadzu FT-IR-8400), X-ray diffraction (XRD) (Malvern panalytical), and UV-visible spectroscopy (Shimadzu UV-160A) and Flame Atomic Absorption Spectroscopy (FAAS) (Phoenix 986, USA).

Preparation of Capsicum Annuum Powder

Leaves of Capsicum annuum were collected, rinsed with water, and air-dried for several days. Subsequently, the leaves are pulverized into a fine powder.

Preparation of Capsicum Annuum Crude Extract

100 mL of deionized water was combined with 10 g of powdered leaves in a 150 mL beaker. The mixture was stirred for two hours at 50 °C. The resultant combination was filtered and dried in a ceramic basin. 0.1 g of collected precipitate was dissolved in 100 mL of deionized water to achieve a concentration of 1000 ppm of leaf extract [34].

General Procedure for Preparation of Silver Nitrate ($AgNO_3$)

0.063 g of $AgNO_3$ was dissolved in 20 mL of deionized water, and the volume was adjusted to 200 mL to prepare a 200 ppm $AgNO_3$ solution.

Green Synthesis of Ag Nanoparticles (AgNPs)

3 mL (1000 ppm) of Capsicum annuum leaves extract was added to 15 mL (200 ppm) of $AgNO_3$ solution, and the mixture was agitated for two h at 60 °C. The color transformation from colorless to brown indicates the formation of AgNPs. The separation of AgNPs was conducted via centrifugation at 11,000 rpm to isolate the nanoparticles and conservation of it in of deionized water.

Synthesis of Polypyrrole

Ppy was produced through the chemical oxidative polymerisation of pyrrole. Initially, 0.2 M of pyrrole monomer solution was prepared by dissolving 0.71 mL of pyrrole in 50 mL of deionized water and agitating for 15 min. Ammonium persulfate (APS) 0.25 M was prepared by adding 50 mL of hydrochloric acid (0.2 M) to 2.85 g of APS, which was then added dropwise to a pyrrole solution over a period of 30 min. The reaction mixture was thereafter agitated for 2 h at ambient temperature to finalize the polymerization. Upon completion of the reaction, the resultant black precipitate was filtered and subsequently washed multiple times with deionized water and ethanol. Finally, the resulting Ppy was dried [35,36].

Preparation of Ppy/ Picric acid/ AgNPs (250) ppm Nanocomposites

Ppy (0.05 g), picric acid (0.39 g), and AgNPs (250 ppm) were placed inside a 10 mL Teflon hydrothermal autoclave. The hydrothermal autoclave was strongly closed and placed in an electric furnace, where it was heated to 180 °C for 6 h [37], to synthesize Ppy/picric acid/ AgNPs nanocomposites. Other composites (Ppy (0.05) g /AgNPs (250) ppm) and (Ppy/ picric acid (0.39) g) were prepared in the same method.

Preparation of Ppy/AgNPs Composite Films (Modification of Electrode)

The spray drying technique was employed to fabricate nanofilms. In this process, 500 microliters of Ppy/AgNPs

nanocomposites are atomized through a nozzle onto ITO glass slides (2×1 cm), where the droplets are concurrently dried on a hot plate to yield the nanofilms. The other nanocomposite films were synthesized in the same method.

Results and Discussion

Synthesis of Silver Nanoparticles

Forming AgNPs Ag^{o} caused by reduction processes between the solution of $AgNO_3$ and the extract of Capsicum annuum leaves, so the colour shift of the mixture from colourless to brown verified the reduction and nanoparticles construct [38]. Fig. 1 suggests a process that may be used to explain the biogenesis of AgNPs.

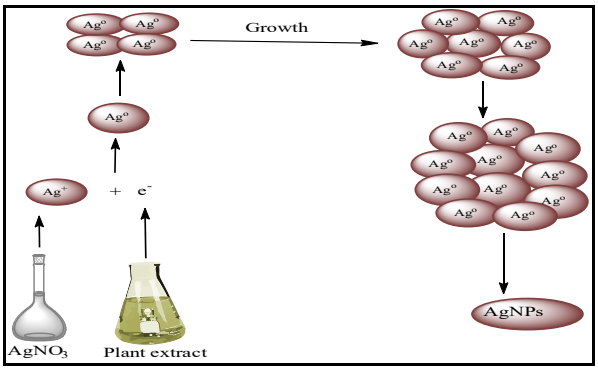

Figure 1. **Mechanism for the synthesis of AgNPs**

Synthesis of Polypyrrole

Using the chemical oxidative polymerization method, Ppy is made by adding APS, which was previously prepared and used as an oxidant for pyrrole monomer, under stirring for 2 h at room temperature with hydrochloric acid as a dopant, as indicated in the Equation.

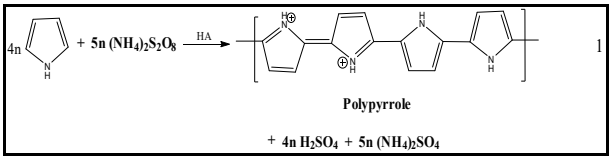

Equation: **Preparation of polypyrrole [36]**

Characterization

Flame Atomic Absorption Spectroscopy

The concentration of produced nanoparticles was quantified by Flame Atomic Absorption Spectroscopy [39], which elucidates that the concentration of AgNPs was 1400 ppm.

Measurement of UV-Visible spectroscopy

UV-visible spectroscopy was used to analyze the produced solution of AgNPs and characterize it. A wide peak at 432 nm was evidence of AgNPs manufacture using leaf extract, as shown in Fig. 2.

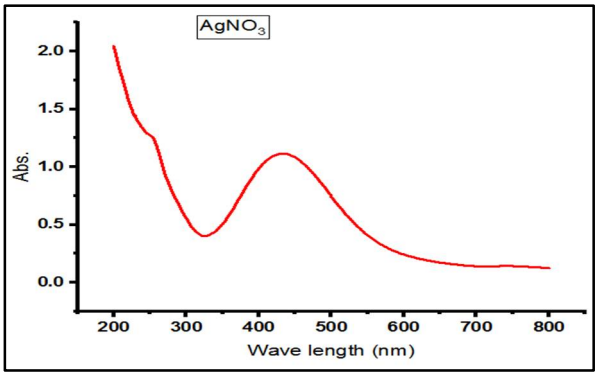

Figure 2. **UV-Visible spectrum for AgNPs**

X-ray diffraction analysis (XRD)

X-ray diffraction methods play a crucial role in the analysis of crystalline and amorphous materials by supplying information pertinent to phase identification. The X-ray diffraction of the synthesized AgNPs utilizing leaf extract is illustrated in Fig. 3. The diffraction peaks located at 2θ = 38.48, 46.56, 64.75, and 77.12 correspond to the (111), (200), (220), and (311) planes, respectively, confirming that the face-centered cubic (fcc) structure of AgNPs (JCPDS file No. 04-0783). According to Debye-Scherer's equation, the mean crystallite size is 22.90 nm. The XRD pattern included supplementary unassigned peaks at 2θ 28.16, 32.58, 55.19,

and 57.82. These peaks were ascribed to the crystalline characteristics of the bio-organic phase (capping agent) on the surface of the AgNPs [40]. Alternatively, it may be attributable to the creation of silver oxide (Ag_2O). Krishnamoorthy et al. observed analogous results [41].

The XRD patterns confirm the inclusion of NPs in the composites, as illustrated in Fig. 4. The XRD pattern of Ppy/AgNPs (250) ppm exhibited a unique reflection positioned at 2θ = 24.49, attributed to the doped Ppy structural properties [42]. The peaks of diffraction at 2θ = 37.58, 43.79, 64.05, 76.55, and 81.14, corresponding to the (111), (200), (220), (311), and (222) planes of silver (Bragg reflection) respectively, and are in agreement with those reported for silver nanoparticles (JCBDS 03-0921) [43]. The sharp XRD peaks of Ag in the composite indicate that the AgNPs are orderly distributed in the composites.

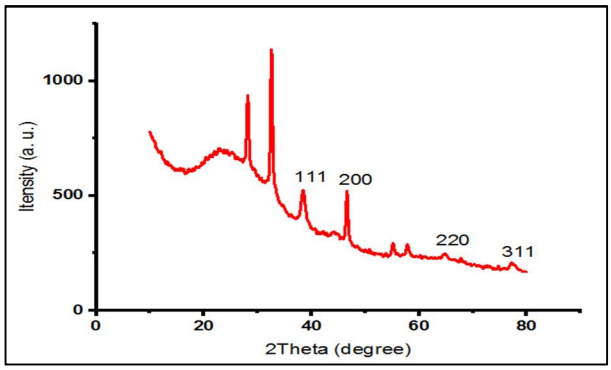

Figure 3. **X-ray diffractogram of AgNPs**

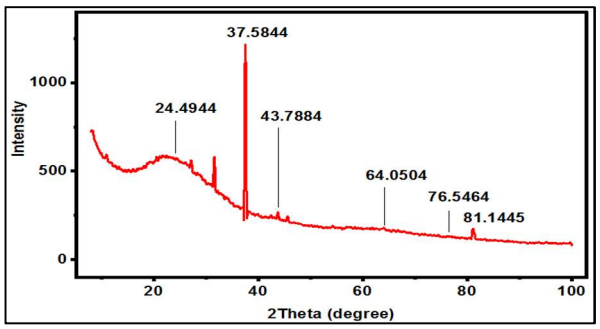

Figure 4. **X-ray diffractogram of Ppy/AgNPs nanocomposites**

Analysis of Fourier Transform Infrared Spectroscopy (FT-IR)

One crucial method for identifying the functional groups of potential biomolecules in the leaf extract is FT-IR spectroscopy. It is in charge of capping these nanoparticles and reducing the metal ions [44]. The FTIR absorption spectrum showed an absorption band at 3275.67 cm^{-1} due to the stretching vibration of the ˛OH group in the dried leaves extract, indicating the presence of phenolic compounds, and might alternatively be ascribed to the (N-H) group. The band at 2926.44 cm^{-1} was attributed to the stretching vibration of the aliphatic C-H group. The presence of C=C groups was demonstrated by the absorption bands at 1645.36 cm^{-1}. The C-H rocking for the alkenes group is responsible for the band at 1384.93 cm^{-1}. The band at 1263.87 cm^{-1} is attributed to the C-O-H. The strong peak observed at 1027.62 cm^{-1} can be attributed to -C-O-C for ether groups [45]. All these regions are shown in Fig.5.

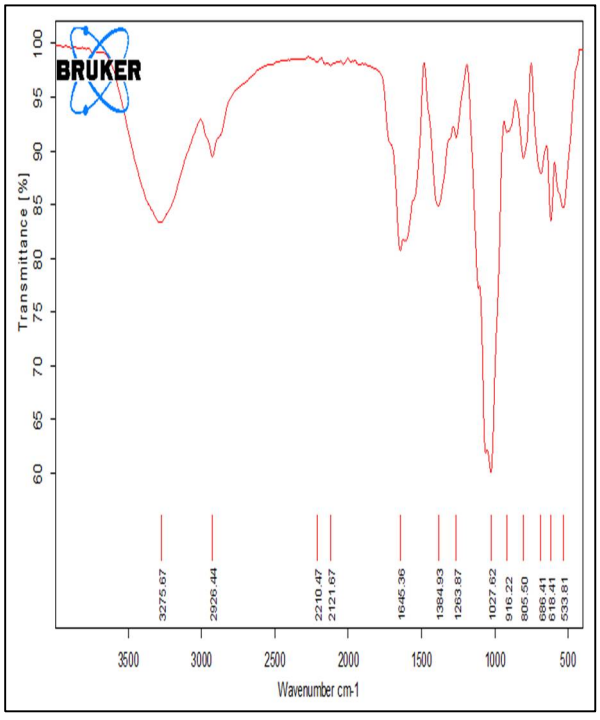

Figure 5. **FT- IR spectrum for leaf extract.**

Field Emission Scanning Electron Microscopy (FESEM)

FESEM is an analytical method utilized to analyze the average size and morphology of nanoparticles inside a sample. FESEM picture of AgNPs synthesized using leaf extract revealed that the nanoparticles exhibit spherical morphology, with a diameter ranging from 31.57 to 42.41 nm, as shown in Fig. 6. The FESEM image of Ppy illustrated the morphology of synthesized Ppy using APS solution. According to the FESEM image, the average diameter ranges from (139.1- 442.3 nm), and the images exhibit a cauliflower-like shape composed of microspherical grains [46], with an average size of 53.05-93.32 as illustrated in Fig. 7. FESEM can be utilized to examine the dimensions and aggregation of nanoparticles within composites. The scanning electron micrographs of Ppy/AgNPs composites are shown in Fig. 8.

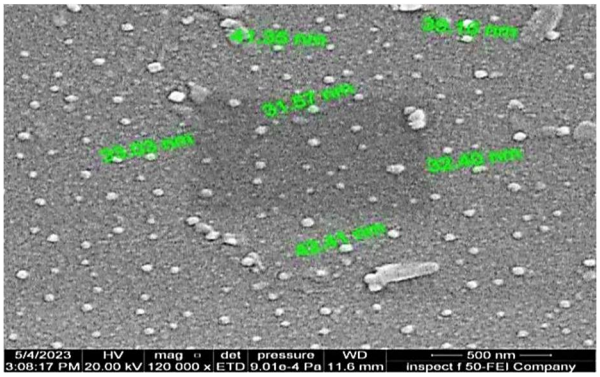

Figure 6. **FESEM Image of AgNPs**

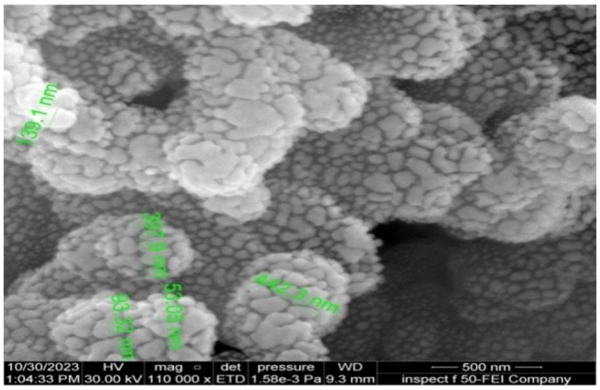

Figure 7. **A FESEM Image of polypyrrole**

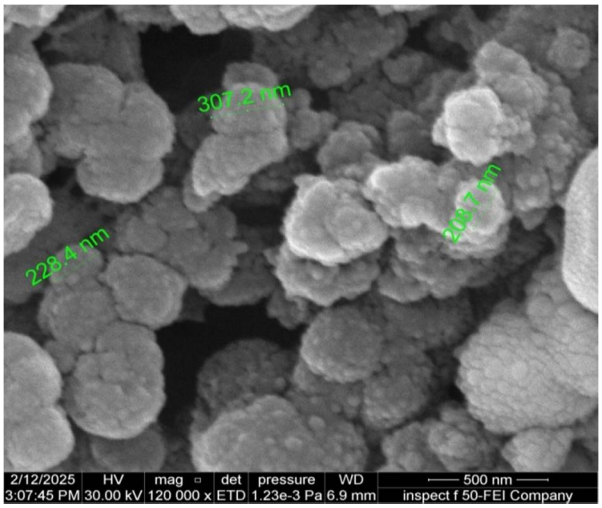

Figure 8. **FESEM images of Ppy/AgNPsnanocomposite**

FESEM images of PPy/AgNPs nanocomposites are spherical in shape with a diameter in the range of 208.7-307.2 nm. Clearly represents that the average grain size is 46.65- 70.80 nm. The surface morphology of PPy/pic nanocomposite was revealed by FESEM micrographs, as shown in Fig. 9. The FESEM images of the nanocomposite showed a slight change in the morphology of PPy after mixing it with pic. According to the FESEM image, the average diameter ranges from 149.1 to 357.2 nm, and the images exhibit a cauliflower-like shape composed of microspherical grains with an average size of 66.06 [46].

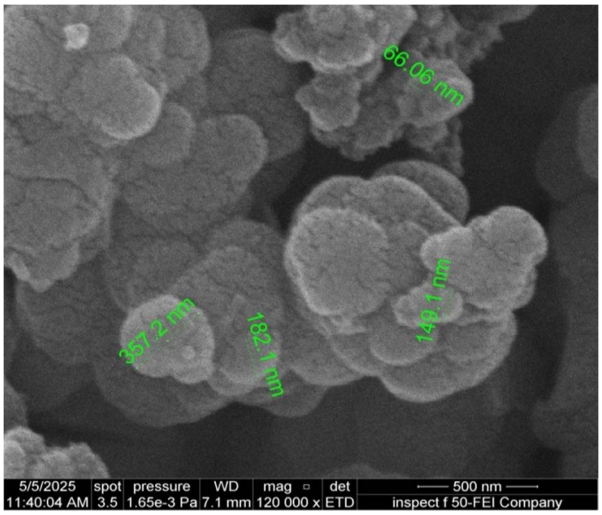

Figure 9. **FESEM of Ppy/ picric acid nanocomposites**

Electrochemical Sensing of Creatinine

The characterization of redox systems is frequently conducted by cyclic voltammetry (CV). This device can store information, including the number of redox states and its stability [47]. The supporting electrolyte is a hydrochloric acid solution (0.1 M).

Fig. 10 illustrates the CVs of creatinine (1 mg/dL) analyzed using a pure PPy film in an acidic solution, revealing the emergence of two pairs of current peaks (oxidation/reduction peaks). The current value of the oxidation peak is (3.44 µA) at potential (-0.075 V), and the reduction peak value is (-4.22 µA) at potential (-0.425 V).

The PPy/AgNPs composite film was utilized for the detection of creatinine (1 mg/dL), as illustrated in Fig. 11. The CV indicated an increase in the peak of the current value. Anodic peak current value (122 µA) at potential (0.120 V) and a cathodic peak current value (-19 µA) at potential (-0.36 V). The increased peak current resulting from the incorporation of AgNPs into Ppy electrodes improves their conductivity.

The produced Ppy/picric acid composite film was utilized for the detection of creatinine in an acidic solution. CVs with a variety of creatinine concentrations (0.2, 1, 5 mg/dL) are shown in Fig. 12. The CV displayed a singular peak of current, and it can be seen that the increase of creatinine concentration causes an increase in peak currents of the Ppy/picric acid electrode. The current values (1.145, 1.876, 2.524) mA at potential (-485, -485, -470) mV, for creatinine (0.2,1,5) mg/dL, respectively. This is related to the reaction of picric acid with creatinine [48].

The produced Ppy/pic/AgNPs (250) ppm films were utilized for the sensing of creatinine in an acidic medium. CVs with a variety of creatinine concentrations (0.2, 0.6, 1, 3, 5 mg/dL) are shown in Fig. 13. The CV showed an increase in peak currents with an increase in creatinine concentration. The current values (oxidation, reduction) ((23.11,-37.77), (53.65, -46.69), (73.19, -61.03), (115, -65.81), (120.9,-56.79)) µA at potential ((0.13,-0.092), (0.13, -0.01), (0.12,-0.082), (0.08, -0.12), (0.02, -0.072))V for (0.2,0.6, 1, 3, 5) mg/dL, respectively. This confirms the improving of sensitivity of the electrode when incorporating AgNPs with Ppy.

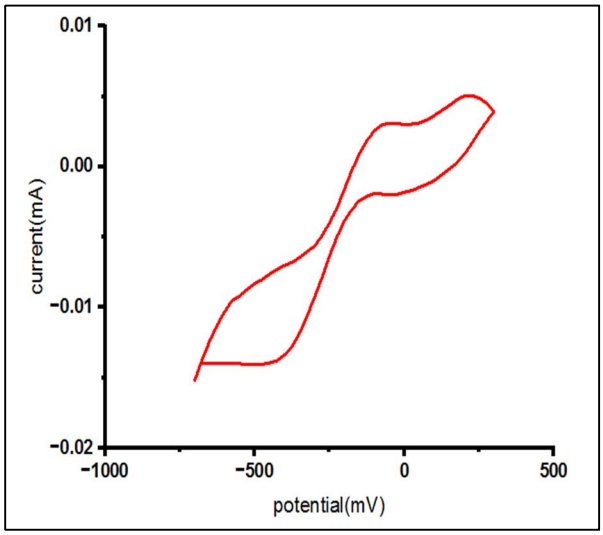

Figure 10. **CV of creatinine (1 mg/dL) using pure Ppy**

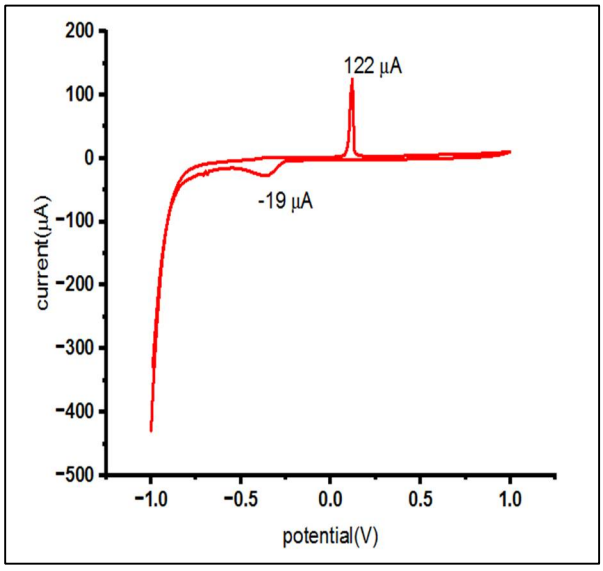

Figure 11. **CV of creatinine using Ppy/AgNPs**

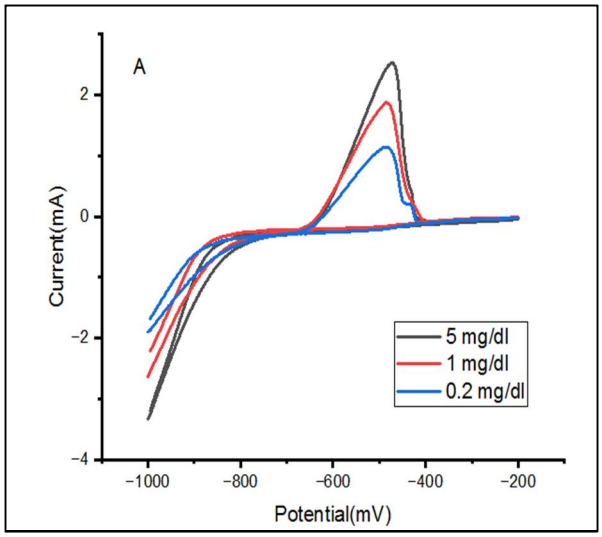

Figure 12. **CV of creatinine using Ppy/picric acid**

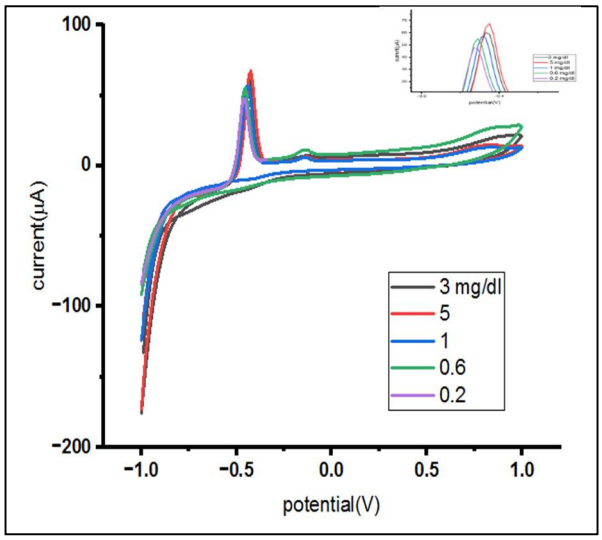

Figure 13. **CV of different concentrations of creatinine with Ppy/pic/AgNPs (250) film**

Interference study

The selectivity of the WE was tested towards potential interferents, such as glucose, urea, and uric acid. When using Ppy/AgNPs electrode, the cyclic voltammograms of glucose (1 mg/dL), Urea (1 mg/dL), and Uric acid (1 mg/dL) in an acidic solution show the disappearance of any peak of current (oxidation or reduction peaks). Which indicate that this electrode does not respond to these materials as illustrated in Fig. 14.

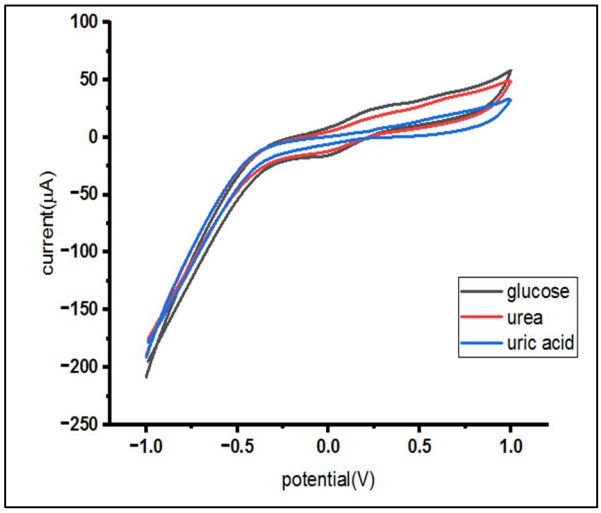

Figure 14. **CV of glucose, urea and uric acid with Ppy/pic/AgNPs (250) film**

Table 1. **The comparison performance of creatinine sensing.**

Electrode	Linear range mM	Sensitivity μAmM^{-1}	Ref.
Glassy carbon macrodisc	0-10 mM	6.09	[49]
PTSPCE/ CuNPs	0.01-0.16 mM	0.2582	[50]
NPG/GCE electrode.	0.01-2 mM	195.05	[51]
SPE electrode	0.37-3.6 mM	16.7	[52]
Ppy/picric acid	0.044-0.22 mM	1830.51	This work
Ppy/pic./ AgNPs (250) ppm	0.0087-0.22 mM	48.82	This work

Conclusions

Creatinine can be identified in various electrochemical biosensors. The determination of creatinine was successfully executed using working electrodes synthesized in various ways. The type of electrode employed for the detection of creatinine influences the resultant current signals, which vary based on the interaction of creatinine with the substance

utilized for the manufacture of the working electrode. The working electrode composed of pure polypyrrole exhibits two minor current peaks. While the working electrode modification with AgNPs enhanced charge transfer efficiency, resulting in amplified analytical signals and elevated current peak values. The working electrode synthesized from polypyrrole and picric acid exhibited a single current peak with a high value, but the working electrode synthesized from polypyrrole, picric acid, and AgNPs had one distinct current peak of varying values, which increased with the increase of creatinine concentration.

Conflict of Interest

?

References

1. T. Nezakati, A. Seifalian, A. Tan and A. M. Seifalian, *Chem. Rev.,* 118 (2018) 6766. https://doi.org/10.1021/acs.chemrev.6b00275.
2. N. Singh, *Polym. Bull.,* 79, (2022) 6929. https://doi.org/10.1007/s00289-021-03840-5.
3. R.B. Choudhary, S. Ansari and B. Purty, *J. Energy Storage,* 29 (2020) 101302. http://dx.doi.org/10.1016/j.est.2020.101302
4. E. N. Zarea, T. Agarwal, A. Zarepour, F. Pinelli, A. Zarrabi, F. Rossi, M. Ashrafizadeh, A. Maleki, M. A. Shahbazi, T. K. Maiti, R. S. Varma, F. R. Tayi, M. R. Hamblin, V. Mattoli and P. Makvandi, *Appl. Mater. Today,* 24 (2021) 101117. https://doi.org/10.1016/j.apmt.2021.101117.
5. S. M. Merdas, A. K. Zaid and Z. M. Kareem, *J. Edu. Pure Sci. Univ. Thi-Qar,* 11 (2021) 1. https://doi.org/10.32792/jeps.v11i1.87.
6. G. K. Raj, E. Singh, U. Hani, K.V.R.N.S. Ramesh, S. Talath, A. Garg, K. Savadatti, T. Bhatt, K. Madhuchandra and R. A.M. Osmani. *J. Control Release,* 355 (2023) 709. https://doi.org/10.1016/j.jconrel.2023.02.017.
7. M.Ding, G. Chen, W. Xu, C. Jia and H. Luo, *Nano Mater. Sci.,* 2 (2020) 264. https://doi.org/10.1016/j.nanoms.2019.09.011.
8. Y Monga, P Kumar, R. K. Sharma, J. Filip, R. S. Varma, R. Zbořil and M. B. Gawande, *ChemSuschem,* 13 (2020) 3288. https://doi.org/10.1002/cssc.202000290
9. A. K. Rashwan, H. Bai, A. I. Osman, K. M. Eltohamy, Z. Chen, H. A. Younis, A. Al-Fatesh, D. W. Rooney and P-S Yap, *Environ. Chem. Lett.,* 21 (2023) 3351. http://dx.doi.org/10.1007/s10311-023-01639-6.
10. E.. Kim, S.Y. Lee, D.Y. Baek, S.Y. Park, S.G. Lee, T. H. Ryu, S.K. Lee, H. J. Kang, O. H. Kwon, M. Kil and S. W. Oh, *Appl. Biol. Chem.,* 62 (2019) 1. https://doi.org/10.1186/s13765-019-0456-y.
11. V. C. Lemos, J. J. Reimer and A. Wormit, *Agriculture,* 9 (2019) 81. https://doi.org/10.3390/agriculture9040081.
12. A. B. Atalay and A.L. Inanc, *Türk Tarımve Doğa Bilimleri Dergisi,* 7 (2020) 132. https://doi.org/10.30910/turkjans.680032.
13. N. P. U. Nguyen, N. T. Dang, L. Doan and T. T. Nguyen, *Processes,* 11 (2023) 2617. https://doi.org/10.3390/pr11092617.
14. A. Dhaka, S. C. Mali, S. Sharma and R. Trivedi, *Results Chem.,* 6 (2023) 101108.

https://doi.org/10.1016/j.rechem.2023.101108.
15. F. Arshad, G. A. Naikoo, I. U. Hassan, S. R. Chava, M. El-Tanani, A. A. Aljabali and M. M. Tambuwala, *Appl. Biocem. Biotechnol.,* 196 (2024) 3636. https://doi.org/10.1007/s12010-023-04719-z.
16. H. B.Ahmed, N. Saad and H.E. Emam. *Surf. Interf.,* 25 (2021) 101175. https://doi.org/10.1016/j.surfin.2021.101175
17. T. Biswal, S. K. BadJena and D. Pradhan, *Mat. Today: Proceed., 30* (2020) 305. https://doi.org/10.1016/j.matpr.2020.01.567.
18. M. K. Egbo, *J. King Saud Uni. Eng. Sci.,* 33 (2021) 557. https://doi.org/10.1016/j.jksues.2020.07.007.
19. B. F. Abdallaha, M. A. Younus and I. J. Ibraheem, *Nanomed. Res. J.,* 6(4) (2021) 369. https://doi.org/10.22034/nmrj.2021.04.007.
20. P. Tetyana, P. M. Shumbula, Z. N. Tetyana, *Intech. Open: London,* UK, (2021). http://dx.doi.org/10.5772/intechopen.97576
21. V. Naresh and N. Lee. *Sensors,* 21 (2021) 1109. https://doi.org/10.3390/s21041109.
22. H. Kaur, A. Bhosale and S. Shrivastav, *Int. J. Health Sci. Res.,* 8 (2018) 315.
23. T. Sawaira, A. Jamil, S. Aziz, A. Mujahid, T. Hussain and A. Afzal, A. *Compos. Commun.,* 37 (2023) 101398. https://doi.org/10.1016/j.coco.2022.101398.
24. A. Singh, A. Sharma, A. Ahmed, A. K. Sundramoorthy, H. Furukawa, S. Arya and A. Khosla, *Biosensors,* 11 (2021) 336. https://doi.org/10.3390/bios11090336.
25. J. Wu, H. Liu, W. Chen, B. Ma, H. Ju, Device integration of electrochemical biosensors. *Nat. Rev. Bioeng.,* 1 (2023) 346. https://doi.org/10.1038/s44222-023-00032-w.
26. B. Razaei, Z. Hassani, M. Shah shahanipour, G. Mohammadnezhad and A. A. Ensafi, *Luminescence,* 33, (2018) 1377. https://doi.org/10.1002/bio.3558.
27. W. Deng, Y. Zhou, A. Libanori, G. Chen, W. Yang and J. Chen. *Chem. Soc. Rev.,* 51 (2022) 3380. https://doi.org/10.1039/D1CS00858G.
28. Z. Saddique, M. Faheem, A. Habib , I. U. l. Hasan, A. Mujahid and A. Afzal, *Diagnostics,* 13 (2023) 1737. https://doi.org/10.3390/diagnostics13101737.
29. T. Sawaira, A. Jamil, S. Aziz, A. Mujahid, T. Hussain and A. Afzal. *Compos. Commun.*, 37 (2023) 101398. https://doi.org/10.1016/j.coco.2022.101398.
30. X. Gao, R. Gui, H. Guo, Z. Wang and Q. Liu, *Sens. Actuat. B Chem.,* 285 (2019) 201. https://doi.org/10.1016/j.snb.2019.01.057.
31. M. J. Pedrozo-Peñafiel, T. Lópes, L.M. Gutiérrez-Beleño, M.E.H.M. Da Costa, D.G. Larrudé and R.Q. Aucelio, *J. Electroanal. Chem.,* 878 (2020) 114561. https://doi.org/10.1016/j.jelechem.2020.114561.
32. R. Sriramprabha, M. Sekar, R. Revathi, C. Viswanathan and J. Wilson, *Anal. Chim. Acta,* 1137 (2020) 103. https://doi.org/10.1016/j.aca.2020.09.004.
33. E. L. Fava, T. M. do Prado, A. Garcia-Filho, T. A. Silvaa, F. H. Cincotto, F. C. de Moraes, R. C. Faria and O. Fatibello-Filhoa, *Talanta* 207 (2020) 120277.

https://2010.1016/j.talanta.2019.120277
34. A. Santhosh, V. Theertha, P. Prakash, and S. S.Chandran, *Mater. Today: Proceed.*, 46 (2021) 4460. http://dx.doi.org/10.1016/j.matpr.2020.09.68.
35. A. S. Abbood and I. J. Ibraheem, *Baghdad Sci. J.,* 21 (2024) 15. https://doi.org/10.21123/bsj.2023.8057.
36. Y. Wang, R. Song , L. Li, R. Fu, Z. Liu and B. Li, *Appl. Sci.,* 12 (2022) 58. https://doi.org/10.3390/app12010058.
37. S. Liu, W. Zeng, Q. Guo and Y. Li, *J. Mater. Sci.: Mater. Electron.,* 31 (2020) 16111. https://link.springer.com/article/10.1007/ 020-s10854-04239-0.
38. S. Jabeen, R. Qureshi, M. Munazir, M. Maqsood, M. Munir, S. S. Hussain Shahand B. Z. Rahim, *Mater. Res. Expr.,* 8 (2021) 092001. https://doi.org/10.1088/2053-1591/ac1de3.
39. B. A. Mahmood, H. H. Meteab and A. M.Jubair, *Int. J. Environ. Impacts,* 8 (2025) 1. http://creativecommons.org/licenses/by/4.0/
40. R. B. Patil and A. D. Chougale, *Mater. Today Proceed.,* 47 (2021). https://doi.org/10.1016/j.matpr.2021.03.384.
41. K. Krishnamoorthy, S. Jayaraman, R. Krishnamoorthy, S. Manoharadas, M. A. Alshuniaber, B. Vikas, V. P. Veeraragh- avan, *J. King Saud Univ. Sci.,* 35 (2023) 102955. https://doi.org/10.1016/j.jksus.2023.102955
42. N.S. Allen, K.S. Murray and R.J. Fleming, *Synth. Met.,* 87 (1997) 237. https://doi.org/10.1016/S0379-6779(97)80115-4.
43. K. Parajuli, L. N. Khanal, G. C. Ganga, S. Koju, S. Bhujel, D. Khadka, M. L. Sharma, B. Pant and B. R. Poudel, *Chem. Eng.,* 917 (2025) 1. https://doi.org/10.3390/chemengineering9010017.
44. J. Singh and A. S. Dhaliwal, *Environ. Tech.*, 41 (2020) 1520. https://doi.org/10.1080/09593330.2018.1540663.
45. K. Niveditha, T. Sukirtha, *Ind. J. Med. Res. Pharm. Sci.,* 5 (2018) 2349. https://doi.org/10.5281/ZENODO.1209310.
46. E. A. Sanches, S. F. Alves, J. C. Soares, A. M. da Silva, C. G. da Silva, S. M. de Souza and H. O. da Frota, *J. Nanomater,*. 2015 (2015) 1. https://doi.org/10.1155/2015/129678.
47. A. Al Tarbuli, Y. M. Alobaidi and H. N. Abdullah, *AIP Conf. Proceed.,* 2660 (2022) 020125. https://doi.org/10.1063/5.0109477.
48. V. Kumar and K. D. Gill, Basic Concepts in Clinical Biochemistry: A Practical Guide, *Chapter* 18 (2018) 75. http://dx.doi.org/10.1007/978-981-10-8186.
49. K. Ngamchuea, S. Wannapaiboon, P. Nongkhunsan, P. Hirunsit and I. Fongkaew, *J. Electrochem. Soc.,*169 (2022) 020567. http://dx.doi.org/10.1149/19457111/ac5346
50. A. Domínguez-Aragón, A. S. Conejo-Dávila, E. A. Zaragoza-Contreras and R. B. Dominguez. *Chemosensors,* 11 (2023) 102. http://dx.doi.org/10.3390/chemosensors11020102.
51. K. Shang, S. Wang, S. Chen and X. Wang, *Biosensors,* 12 (2022) 588. https://doi.org/10.3390/bios12080588.
52. J. C. Chen, A.S. Kumar, H. H. Chung, S. H. Chien, M. C. Kuo, J. M. Zen, *Sens. Actuators B: Chem.,* 115 (2006) 473. https://doi.org/10.1016/j.snb.2005.10.015.